Article

Optimizing Hot-Work Tool Steel Microstructure for Enhanced Toughness

Anže Bajželj [1,2] , Tilen Balaško [2] , Barbara Šetina Batič [1] and Jaka Burja [1,2,*]

1 Institute of Metals and Technology, Lepi pot 11, 1000 Ljubljana, Slovenia; anze.bajzelj@imt.si (A.B.); barbar.setina@imt.si (B.Š.B.)
2 Faculty of Natural Sciences and Engineering, University of Ljubljana, Aškerčeva Cesta 12, 1000 Ljubljana, Slovenia; tilen.balasko@ntf.uni-lj.si
* Correspondence: jaka.burja@imt.si

Abstract: Hot-work tool steels play a crucial role in applications exposed to extreme thermal, mechanical, and chemical stresses and require exceptional properties such as high strength, hardness, wear resistance, and toughness. The latter is crucial to prevent an unexpected tool failure due to the formation and propagation of fatigue cracks in demanding environments. In addition, high thermal conductivity is crucial to prevent overheating of the tool and the resulting degradation of the material. This study focuses on a new generation hot-work tool steel with increased Mo and W contents, which has excellent thermal conductivity but limited toughness, as it contains stable Mo-W carbides that remain stable up to 1100 °C. To improve toughness, an alternative heat-treatment method involving austempering at different temperatures was applied. The investigation begins with the characterisation of the chemical composition of the steel, followed by the determination of the martensite-start (M_S) and martensite-finish (M_f) temperatures. Based on the results, the researchers established a set of samples for austempering heat treatment. They investigated the effects of different isothermal holding temperatures on the microstructure of the steel and its subsequent mechanical properties. The results show that reduced bainite formation, achieved by austempering at certain temperatures, led to significantly improved impact toughness and moderate hardness. This study also showed a correlation between the isothermal holding temperature and the extent of martensitic transformation, which affected the microstructure and mechanical properties of the steel.

Keywords: hot-work tool steel; austempering; bainitic transformation; lower bainite; impact toughness

1. Introduction

Hot-work tool steels play an important role in applications that are exposed to extreme thermal, mechanical, and chemical stresses, such plastics and metal forming. The most severe environments include aluminium and magnesium high-pressure die casting, aluminium extrusion, and other hot metal-forming processes. These demanding environments require materials with exceptional properties, including high strength, hardness, wear resistance, and, critically, toughness [1–3]. Hot-work tool steels with higher toughness exhibit a resistance to the initiation and propagation of fatigue cracks, which is important in preventing an unexpected tool failure. Consequently, toughness stands as a fundamental property that enhances the durability and performance of hot-work tool steels in high-temperature applications [4–9]. In addition, hot-work tool steels must exhibit high thermal conductivity to facilitate rapid heat dissipation and prevent excessive tool overheating during cycles. Excessive overheating of the tool can lead to more severe fatigue crack formation and material degradation. Pure iron possesses a very high thermal conductivity of approximately 80 W/mK at room temperature, but the addition of alloying elements that enables high mechanical properties reduces the conductivity values significantly. Typically, hot-work tool steels will achieve an average thermal conductivity of around 20 W/mK,

while the novel high thermal conductivity Mo-W tool steels will achieve up to 45 W/mK at room temperature [10–13].

Hot-work tool steels usually undergo a heat treatment process involving quenching and multi-stage tempering. This process results in a tempered martensite microstructure with alloy carbides, and the combination exhibits good mechanical properties, enhanced wear resistance, and ductility. The main objective of austenitisation is to dissolve large carbides and other phases in the austenite matrix; to achieve a sufficiently high carbon content; to ensure hardness, while maintaining the grain growth-retarding precipitates; and to minimize the growth of austenite crystal grains. A fine microstructure is required to fulfil high mechanical properties with good ductility. Following quenching, a multi-stage tempering process is carried out to reduce internal stresses and form finely dispersed secondary carbides that enhance the hardness and toughness of the steel. Insufficient austenitisation leads to the presence of undissolved primary and secondary carbides in the microstructure, which reduce the ductility of hot-work tool steels, because these carbides are typically formed along the boundaries of prior austenitic crystal grains [4,14–22].

Bainite is a possible alternative to the classical tempered martensite. It exhibits a morphology somewhat similar to martensite but with limited carbon diffusion. The formation of bainite can also be described as a military transformation [23]. However, bainite can be more homogeneous with finer, evenly distributed carbides. As a result, the bainitic microstructure in steels can be more ductile while still possessing high strength and hardness compared to the tempered martensitic microstructure [18,23–30]. Due to the lower concentration of residual stresses in the material, the toughness of steels with a lower bainitic microstructure is higher compared to martensite [27,31]. Lower bainite formation in hot-work tool steels is achieved by holding them at temperatures above and below the martensite-start transformation temperature (M_S). Lower temperatures reduce the stability of austenite, leading to the rapid formation of lower bainite. The diffusion of carbon and other alloying elements is restricted, resulting in a fine bainitic microstructure. Martensitic grains that form during cooling below the M_S temperature act as nucleation sites and accelerate the transformation into lower bainite [30,32–34].

In this study, a new generation hot-work tool steel with an increased content of Mo and W was utilised. This steel exhibits exceptional thermal conductivity, a crucial property in the design of tools. However, the analysed hot-work tool steel has a limited toughness, which is the main significant challenge of this hot-work tool steel. A reduced toughness of the hot-work tool steel can be attributed to the presence of stable Mo-W carbides, which remain stable up to 1100 °C [14,35]. Despite high austenitisation temperatures, Mo-W carbides persist within the matrix, and significant grain growth further negatively impacts mechanical properties. To improve toughness, a different heat treatment was applied, involving austempering at various temperatures. This study focuses on the characterisation of the microstructure of the hot-work tool steel after austempering at different temperatures with the aim of determining a more suitable heat treatment to improve the toughness of the steel.

2. Materials and Methods

The delivered tool steel was in a spheroidised thermal state, with its chemical composition given in Table 1. The chemical composition of the steel was determined by optical emission spectroscopy with an ARL 3460 device (Thermo Fisher Scientific, Waltham, MA, USA). Additionally, the carbon, sulphur, and nitrogen contents were determined using a combustion method with ELTRA CS-800 and ELTRA ON-900 (Leco Co., Ltd., St. Joseph, MI, USA).

Table 1. Chemical composition of analysed hot-work tool steel (wt. %).

C	Si	Mn	S	Ni	Mo	W	N	Fe
0.32	0.04	0.02	0.0009	0.03	3.2	1.7	0.001	bal.

Cylindrical shape specimens with a diameter of Ø4 mm × 10 mm were produced to determine the martensite-start (M_S) and martensite-finish (M_f) temperatures using a TA DIL805A dilatometer (TA, New Castle, DE, USA). The samples were heated in a vacuum with a heating rate of 10 °C/s to an austenitising temperature of 1080 °C, held at this temperature for 600 s, and then rapidly cooled by inert gas blowing to the room temperature at a rate of 30 °C/s in an argon atmosphere. The M_S and M_f were determined at 405 °C and at 225 °C, respectively, using the dilatometric cooling curve shown in Figure 1, using the tangent method. The curve is not typical for a martensitic transformation. It starts at relatively high temperatures (405 °C). After three experiments, the results were the same. The presence of bainite was not confirmed in the samples cooled at 30 °C/s, and the deviations occur due to the segregations.
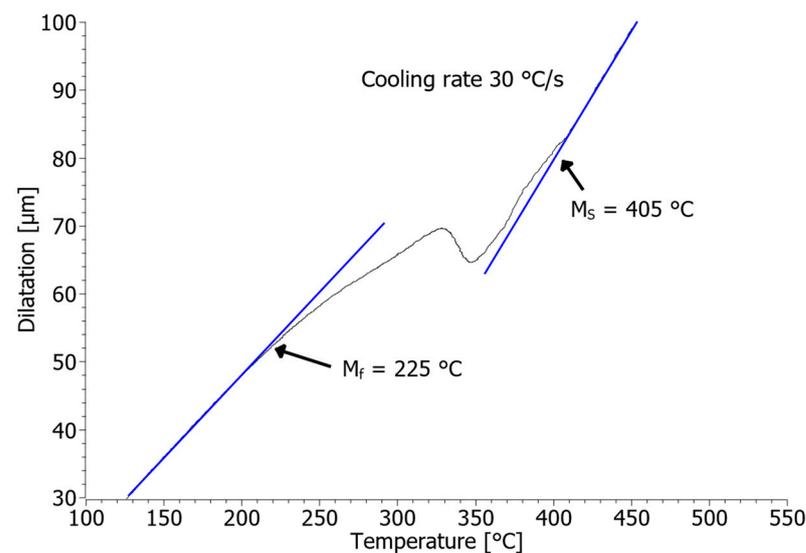

Figure 1. Dilatometer cooling curve of quenched sample from the austenitisation temperature at a cooling rate of 30 °C/s.

Based on the results of the martensitic transformation temperatures, subsequent heat treatment steps were determined. A set of samples was subjected to austempering heat treatment, following the austenitisation process. This involved cooling at the rate of 30 °C/s and isothermal holding of the samples between 300 and 550 °C in an inert argon gas atmosphere for 2 h, followed by rapid cooling to room temperature. Figure 2 illustrates the proposed heat treatment process experiments. Dilatation values were determined during the isothermal holding at selected temperatures using dilatometric curves.

To assess the Charpy V-notch (CVN) impact toughness, larger specimens (65 mm × 15 mm × 15 mm) were subjected to heat treatment experiments involving isothermal holding. Austenitisation of the samples at 1080 °C was conducted in an electric resistance furnace (Nabertherm GmbH, Lilienthal, Germany) followed by rapid cooling in a preheated salt bath, where the samples were held for 2 h between 300 and 550 °C. The isothermal transformation was followed by a rapid cooling of the samples to room temperature. After the heat treatment, standard Charpy V-notch specimens with dimensions of 55 mm × 10 mm × 10 mm, with 2 mm notches, were machined for the Charpy impact test. The Charpy impact measurements were performed at room temperature using a 300 J pendulum.

Samples were prepared for metallographic analysis from dilatometric specimens and samples used for measuring impact toughness. These samples were ground, polished, and etched with Nital (5 vol. %). The characterisation of the microstructure was carried out using a ZEISS Axio Imager Z2M (Carl Zeiss AG, Oberkochen, Germany) optical microscope. Phase characterisation was performed by scanning electron microscopy (SEM) using a Zeiss CrossBeam 550 microscope (Carl Zeiss AG, Oberkochen, Germany). X-ray spectroscopy

(EDS) and electron backscatter diffraction (EBSD) were performed using a HikariSuper EBSD camera (EDAX, Mahwah, NJ, USA). The accelerating voltage for EBSD was 20 kV, the tilt angle was 70°, and the step size was 0.2 μm. Vickers microhardness (HV0.025) and Rockwell hardness (HRC) were measured on metallographic specimens using the Instron Tukon 2100B (Wilson Instruments, Norwood, MA, USA) and Rockwell Series B2000 (Wilson Instruments, Norwood, MA, USA) machines.
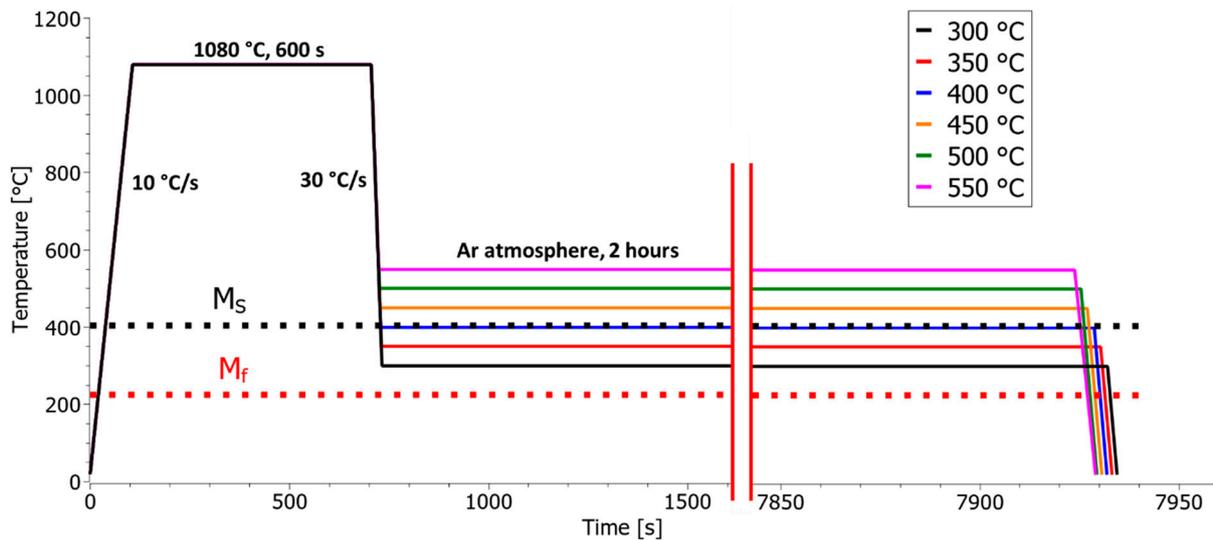

Figure 2. The experimental process in the dilatometer, austenitisation, and different isothermal holding temperatures in inert argon atmosphere, the double red lines present a time gap.

3. Results and Discussion

Figure 3 shows the dilatometric dilatation curves of samples held at isothermal temperatures between 300 and 550 °C. The left side of the graph shows the cooling of the samples to the isothermal holding temperature, while the right side shows the details of the isothermal holding and subsequent rapid cooling to room temperature. For samples held at the isothermal temperatures between 300 and 400 °C, a deviation in the dilatation curve was observed during cooling from the austenitisation temperature to the isothermal temperature, indicating the martensitic transformation of some austenite, as expected from Figure 1. If the isothermal holding temperature is lower than the M_S, it will lead to partial martensite transformation during cooling. When the samples reached the specified temperature, the isothermal transformation to bainite occurred relatively fast. Interestingly, the presence of a small fraction of martensite accelerates the isothermal bainite transformation. As found by Tian et al. [30], Morawiec et al. [32], Pashangeh et al. [33], and Guo et al. [34], due to the shear-like military transformation of martensite, a higher concentration of martensite increases the dislocation density and increases the internal stresses in the undercooled austenite, enhancing the driving force for the nucleation and transformation of bainite. Although they are both classified as military transformations, unlike martensite, bainitic transformation typically requires a nucleation period. As the isothermal temperature increases, less martensite is formed during cooling, and consequently, more bainite is formed during isothermal holding. The isothermal transformation to bainite was complete, and upon cooling to room temperature, there were no visible deviations in the dilatation curve that would represent martensitic transformation. At austempering temperatures above 450 °C, martensitic transformation did not occur during the cooling to the isothermal temperature, which is a logical consequence of the fact that the determined martensitic start temperature was 405 °C. Once the samples had reached the prescribed temperature, a short incubation period followed, after which isothermal transformation to bainite took place. With an increase in the isothermal holding temperature, both the incubation time and the transformation rate decreased. Higher temperatures increased the stability of the

austenite, reduced the nucleation rate for bainite formation, and consequently slowed down or completely suppressed the transformation rate. At higher temperatures, specifically 500 and 550 °C, the transformation into bainite either proceeded slowly throughout the entire holding period or did not occur at all. The isothermal bainite transformation was inhibited due to the stabilisation of the austenite and an insufficient ferrite-forming driving force; therefore, the martensitic transformation took place during the final quenching to room temperature after the isothermal holding. Furthermore, a slight deviation in the dilatometric curve that indicates the start of the martensitic transformation is observed in Figure 1, and this can also be noticed in the first stage of cooling before austempering at 400, 350, and 300 °C and can also be observed during the final cooling stage of samples isothermally held at 550 °C.
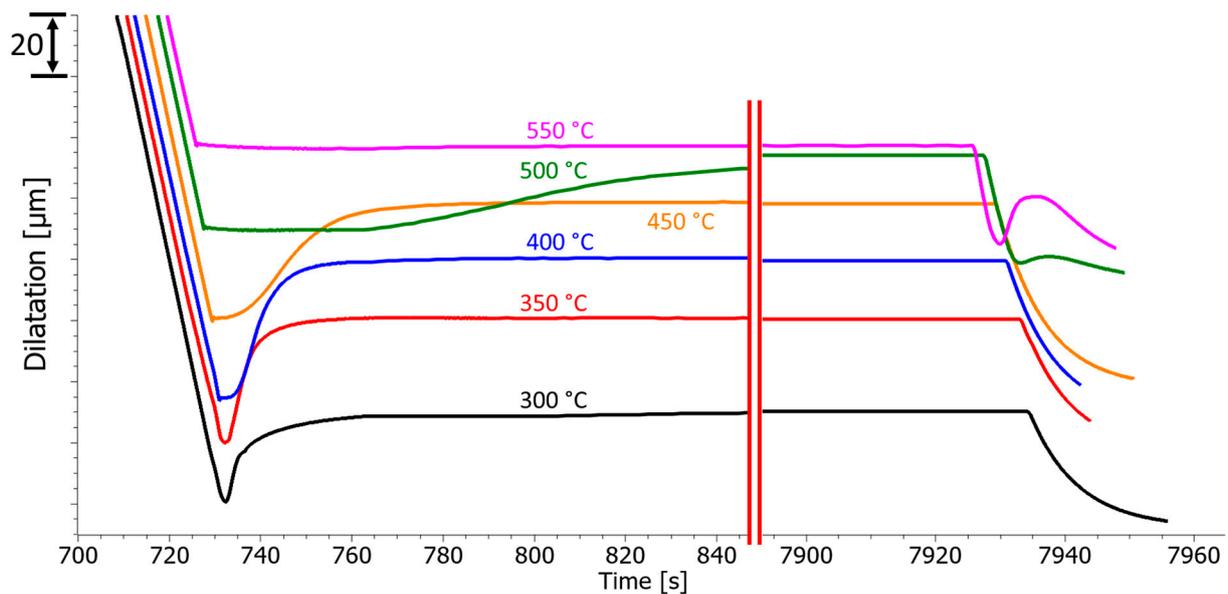

Figure 3. Dilatometric dilatation vs. time curve for the isothermal transformation regimes between 300 and 550 °C (the double red lines present a time gap).

Figure 4 illustrates the absolute elongation of the samples during isothermal holding at various temperatures. For the samples held at an austempering temperature below 400 °C, the martensitic transformation occurred during cooling to the isothermal holding temperature, resulting in less bainite formation as the isothermal temperature decreased. Isothermal bainitic transformations occurred rapidly at these temperatures and were completed within a few seconds. For the sample held at 300 °C, a deviation occurred during cooling to the isothermal temperature, and the sample did not follow the planned trajectory. A step is noticeable on the curve when the sample reached the isothermal temperature. The martensite transformation occurred mainly during cooling, while the isothermal bainite transformation occurred during holding at the specified temperature. For the sample held at 350 °C, a significant portion of the transformation corresponds to an isothermal bainite transformation, and due to the presence of martensite, the transformation occurred within a few seconds. The bainite transformation in the sample held at 400 °C proceeded somewhat more slowly with a short incubation period. The proportion of bainite formation is higher, which is reflected in a greater absolute elongation. During isothermal holding, both martensite and bainite tempered, as can be seen from the change in the elongation curves. The rate of isothermal transformation in the sample held at 450 °C was slower due to the slower nucleation of bainite. The lower absolute elongation indicates the formation of upper bainite. In the sample held at an isothermal temperature of 500 °C, the bainite transformation occurred slowly throughout the entire holding period, whereas in the sample held at 550 °C, no isothermal bainite transformation occurred.
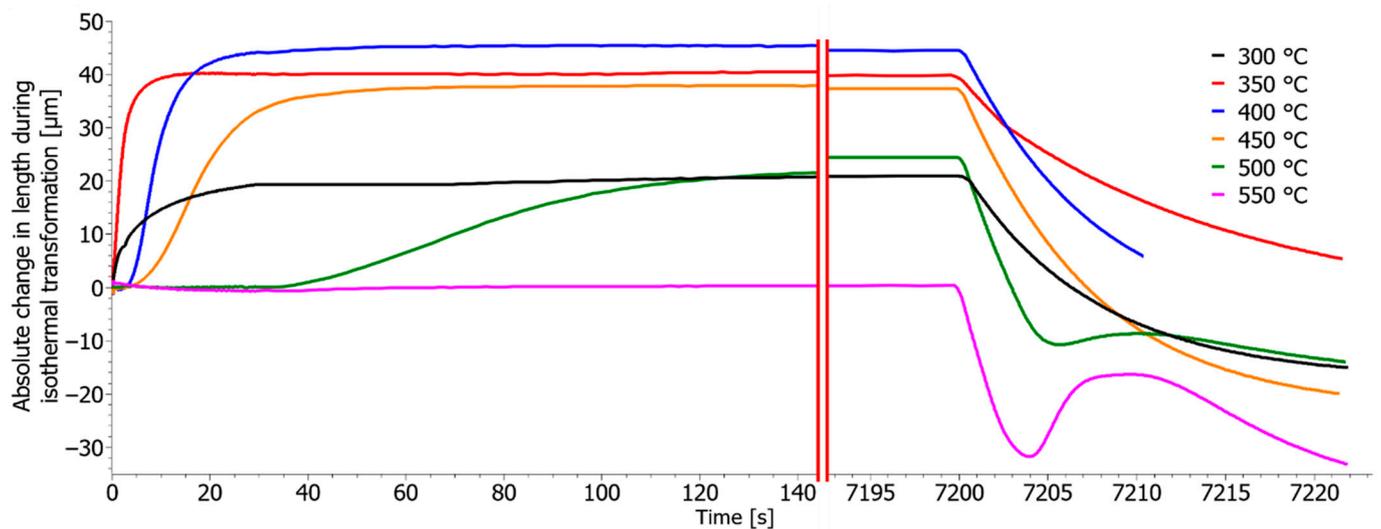
Figure 4. Absolute change in length during isothermal transformation (the double red lines present a time gap).

Figure 5a–f show etched microstructures of samples held at isothermal temperatures between 300 and 550 °C, with labelled phases and the corresponding measured microhardness values (HV0.025). The values of microhardness with such small loads result in higher values than measurements with higher loads. The samples held at isothermal temperatures between 300 and 400 °C contain both lower bainite and martensite. The difference in microhardness between the bainite and the tempered martensite is minimal and could not be distinguished by microhardness measurements. In the sample held at 400 °C, the microstructure contains lower bainite, very little martensite, and upper bainite. In the sample held at 450 °C, the upper bainite dominates the microstructure with the lowest hardness. In the sample held at 500 °C, during isothermal heat treatment, a slow bainitic transformation occurs, and the microstructure shows some upper bainite. Between the bainitic plates, there are laths of martensite, resulting in a higher measured microhardness of bainite. Additionally, fresh martensite forms due to the transformation of stabilised austenite during quenching to room temperature after isothermal holding. A similar process occurred in the sample held at 550 °C, where an isothermal bainitic transformation practically did not occur. The newly formed martensite in these samples has a significantly higher hardness than the martensite formed in the samples held at 300, 350, and 400 °C.

Figure 6a–f show scanning electron microscope images of the examined samples subjected to various isothermal temperatures. Notably, these figures reveal the presence of undissolved carbides, enriched in Mo and W, surrounding the prior austenitic grains in all samples. Figure 7 shows a backscattered electron image of a sample held at 300 °C and carbides rich in Mo and W. These carbides are not as efficient in retaining small austenitic crystal grains such as NbC for example [14]. According to the observations with the optical microscope, the sample held at 300 °C exhibits a significant martensitic phase. However, as the isothermal holding temperature increases, the proportion of bainite becomes more prominent. Lower bainite, characterised by uniformly distributed carbide particles, plays a constructive role in enhancing Charpy impact toughness, a detail that will be presented later in this discussion. As the isothermal holding temperature increased, the morphology of the bainite underwent a noteworthy transformation. This evolution could be attributed to the intensified carbon diffusion originating from the bainitic ferrite plates. The consequence was the formation of carbide particles around these plates, a phenomenon that became especially pronounced in samples held at temperatures exceeding 450 °C. Notably, the sample held at 500 °C exhibits the presence of upper bainite. This occurrence reflected the formation of bainitic ferrite plates, leading to a carbon-enriched zone in the surrounding area, subsequently impacting the stabilisation of the austenite. During the cooling phase to

room temperature, the stabilised austenite underwent a transformation, converting into fresh martensite. As shown from the dilatometric curves, in the sample held at 550 °C, an isothermal bainite transformation practically did not occur, resulting in a predominantly martensitic microstructure. The EBSD phase analysis clearly indicated a comprehensive transformation of austenite to either martensite or bainite across all examined samples, and there were no traces of any retained austenite. Figure 8 presents the EBSD phase analysis of the sample held at 350 °C.
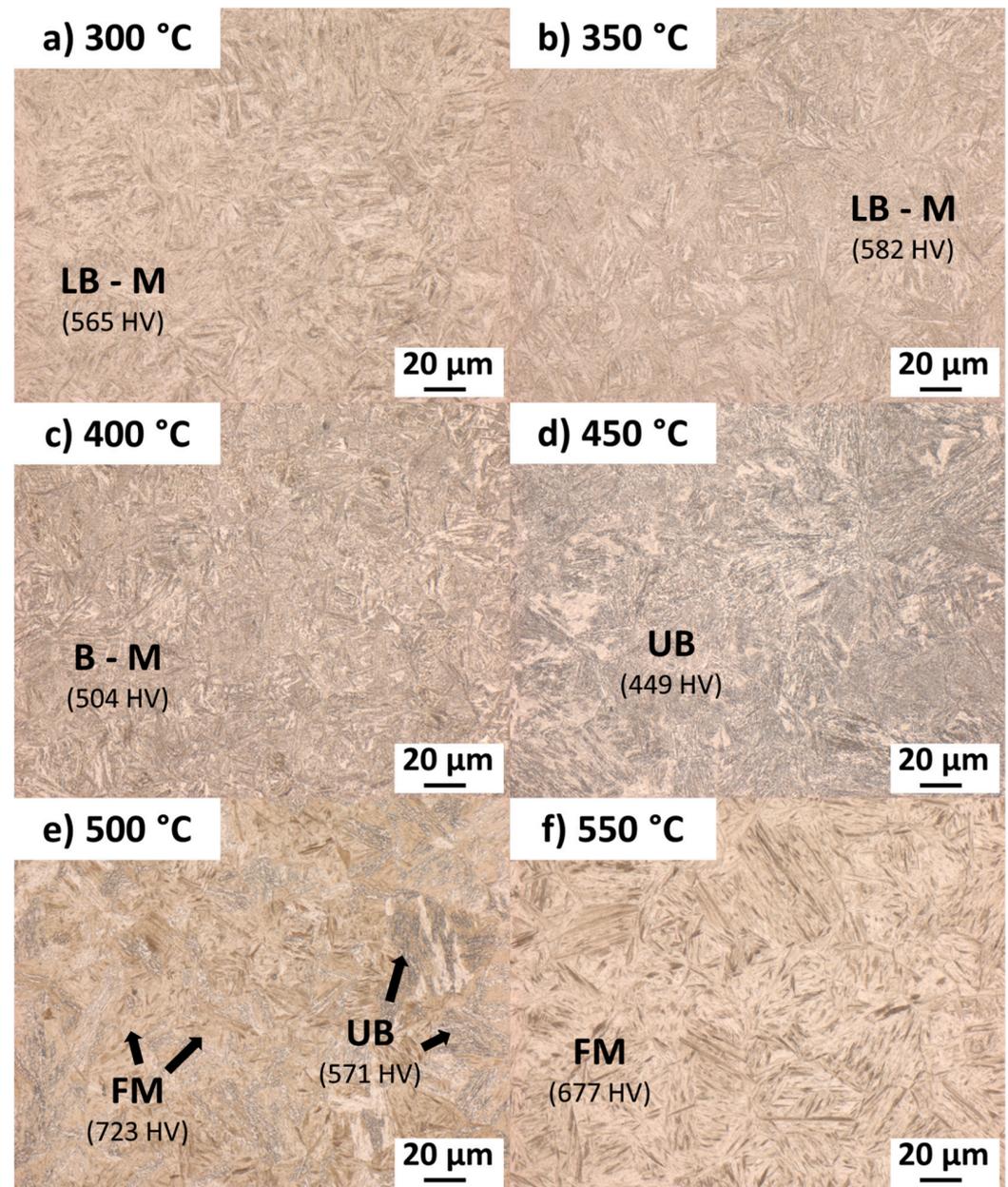

Figure 5. Optical microscopy of etched samples held at different isothermal temperatures: (**a**) 300 °C, (**b**) 350 °C, (**c**) 400 °C, (**d**) 450 °C, (**e**) 500 °C, (**f**) 550 °C. Notes: LB—lower bainite, M—martensite, B—lower or upper bainite, UB—upper bainite, FM—fresh martensite.
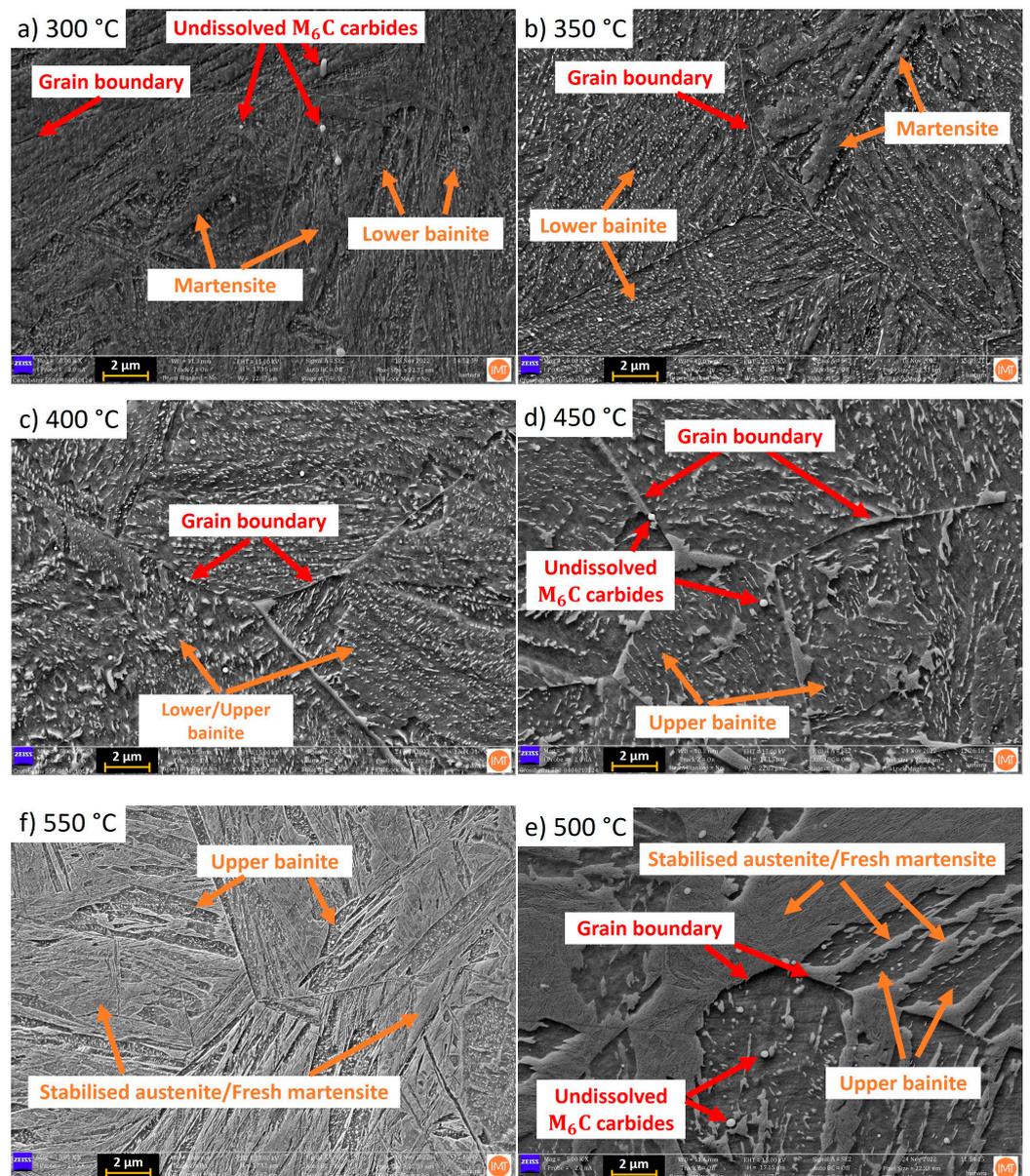
Figure 6. Scanning electron microscopy images of samples held at (**a**) 300, (**b**) 350, (**c**) 400, (**d**) 450, (**e**) 500, and (**f**) 550 °C.
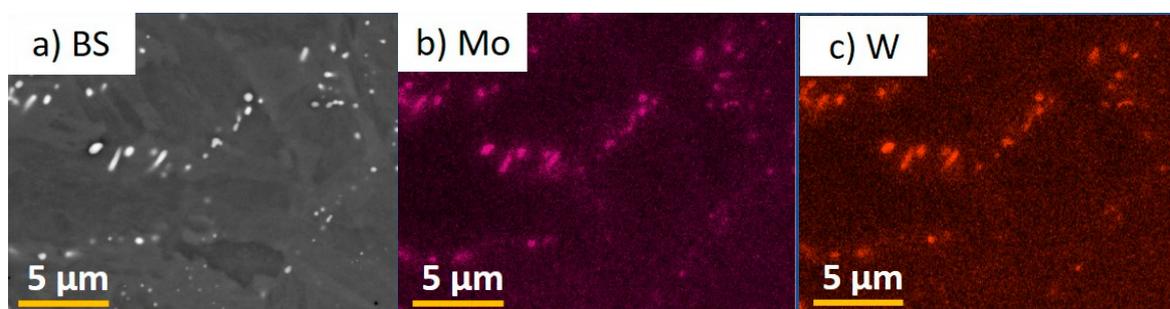

Figure 7. (**a**) Backscattered electron image of sample held at 300 °C and EDS elemental mapping of (**b**) Mo and (**c**) W.

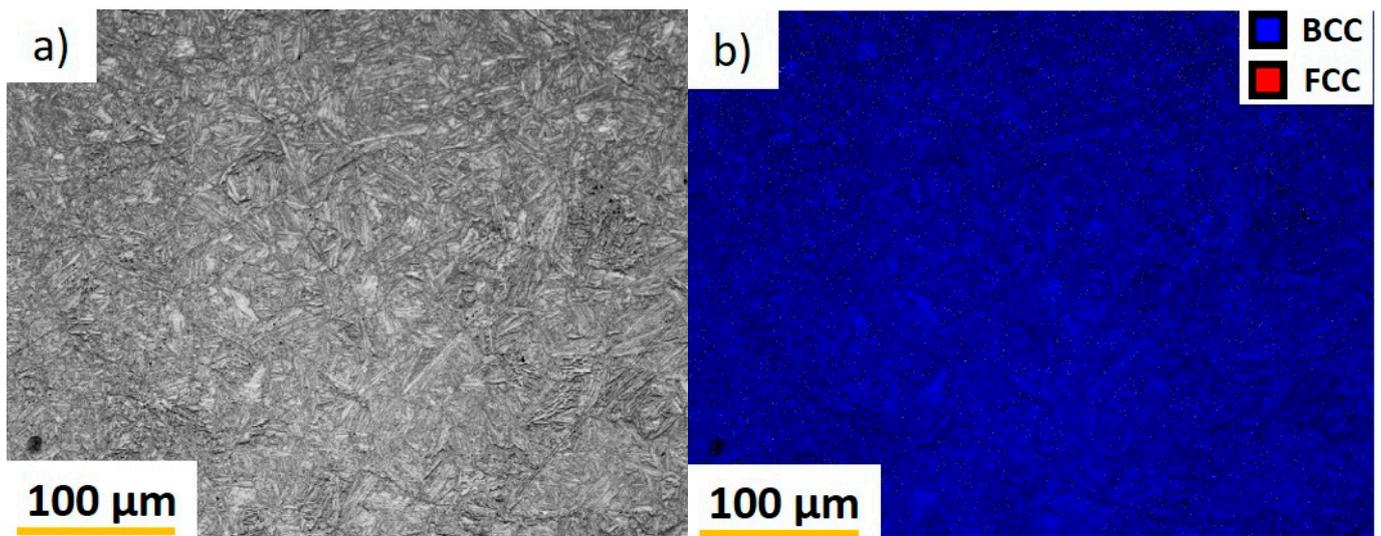**Figure 8.** (**a**) Scanning electron microscopy image of sample held at 350 °C and (**b**) EBSD phase analysis.

Figure 9 shows the results of the Charpy CVN impact toughness and hardness measurements (HRCs). To obtain a more precise determination of the Charpy impact toughness, additional measurements were conducted at the isothermal holding temperatures of 325 and 375 °C. The Charpy impact toughness and hardness measurements were not performed on the sample held at 550 °C due to the absence of bainite. The Charpy CVN impact toughness of the samples after conventional heat treatment (CHT) was 4.5 J. These samples were quenched at a temperature of 1080 °C, followed by triple tempering to a hardness of 47 HRC. Tools for aluminium and magnesium die casting, plastic injection moulding, and hot forging typically achieve hardness levels ranging from 44 to 52 HRC [36]. Through the austempering heat treatment process, the Charpy impact toughness increased with an increase in the isothermal holding temperature, reaching its maximum value of 17.5 J at 350 °C. Subsequently, the Charpy impact toughness values decreased, following a similar trend as hardness. The increase in the Charpy impact toughness and the higher hardness could be due to the higher amount of bainite and the more extensive tempering of martensite and lower bainite. With an increase in the isothermal holding temperature, the presence of martensite or tempered martensite disappeared, being replaced by upper bainite. Consequently, this is reflected in a lower hardness and Charpy impact toughness. For the sample held at 500 °C, the martensitic transformation occurred during cooling from the isothermal temperature to room temperature. The presence of untempered martensite and upper bainite led to the lowest Charpy impact toughness and the highest measured hardness. The austempering method significantly increased the Charpy impact toughness of the investigated hot-work tool steel, with the sample held at a temperature of 350 °C, demonstrating the best results. Notably, hardness levels were lower compared to the samples treated through conventional heat treatment, as the lower bainite did not achieve a comparable hardness to the tempered martensite.
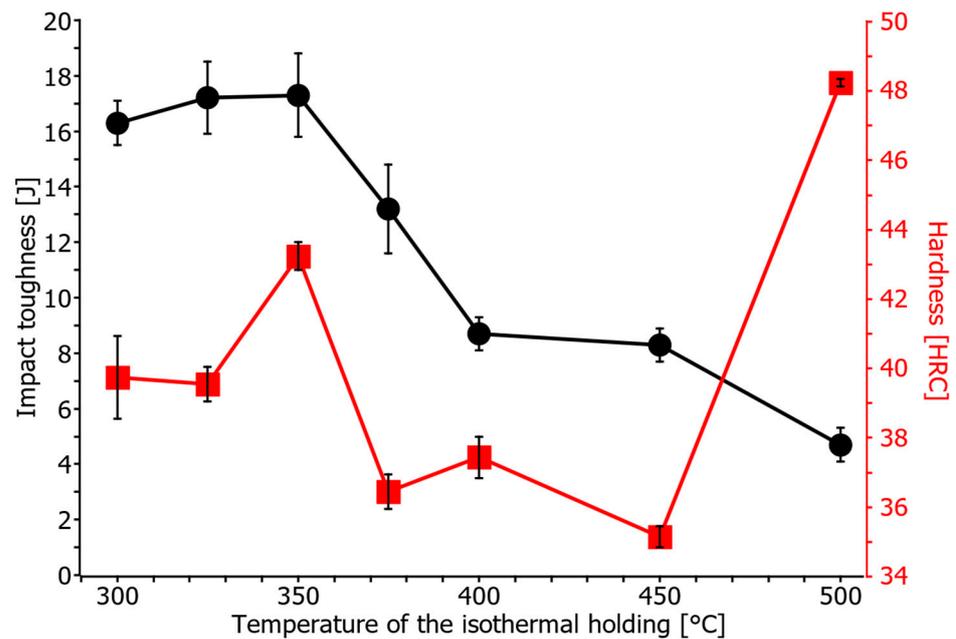
Figure 9. Charpy CVN impact toughness (black line) and hardness measurements (HRCs, red line) at various isothermal holding temperatures.

Figure 10 shows scanning electron microscopy images of the fracture surface after the Charpy impact toughness test of the samples held at 350 °C and 500 °C. The sample held at 350 °C achieved the highest Charpy impact toughness among all the samples but exhibited a brittle fracture. The brittle fracture can be instigated by the residual stresses in martensite, and we tried to mitigate the influence of martensite by introducing bainite. That being said, soft and ductile retained austenite can also improve the Charpy impact toughness of steel [37]. In our case the fracture surface showed small areas characteristic of ductile fracture that were several μm wide (see areas marked with dimples in Figure 10). Because the EBSD analysis did not detect retained austenite on such a scale, it was not considered to be a major factor in the increase in the Charpy impact toughness. Additionally, the majority of the sample fractured surface still exhibits a brittle fracture. This at least partially excludes the possible effect of nano-sized retained austenite between the bainitic needles. While the Charpy impact toughness values are still below 20 J, the values increased for more than 100%. Studies on low-alloyed high-carbon steel showed an increase from 8 J for quenching and tempering to as high as 29 J for austempering [24]. Furthermore, there is still ground for improvement in the process of annealing. Bainitic steels, characterised by the presence of strong carbide-forming elements such as molybdenum (Mo) and tungsten (W), exhibit secondary hardening when subjected to high-temperature annealing. This secondary hardening process can provide higher toughness and hardness. The finely dispersed and more thermodynamically stable alloy carbides replace cementite within the microstructure [23]. The conventionally heat-treated specimens that were quenched and tempered had a high amount of Mo and W carbides, resulting in a relatively high secondary hardness of around 540 HV [15].
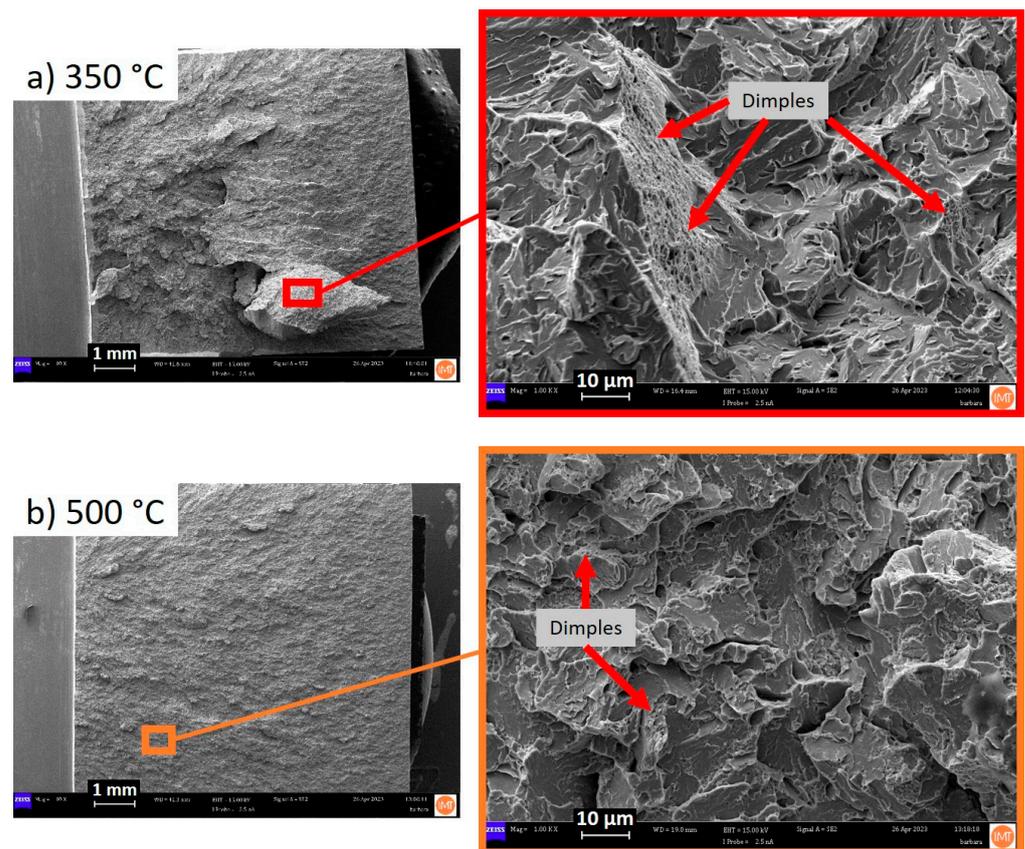
Figure 10. Fracture surface of the samples held at (**a**) 350 °C and (**b**) 500 °C.

4. Conclusions

In this study, heat treatment was optimised with the aim of improving the impact toughness of hot-work tool steels. Instead of the conventional method of quenching and multiple tempering, austempering was carried out at various isothermal temperatures after austenitisation. Based on the microstructural characterisation and the determination of hardness and impact toughness, the following conclusions can be summarised:

- Austempering below the martensite-start transformation temperature (M_S) led to the formation of some martensite during cooling to the isothermal temperature, which was subsequently tempered during isothermal holding. The martensite formed serves as a nucleus for an isothermal bainite transformation. Samples with tempered martensite and lower bainite achieved significantly higher impact toughness values compared to samples treated with conventional heat treatment.
- When the isothermal temperature rose to 450 °C, the morphology of the bainite changed, with more upper bainite forming. An increased proportion of upper bainite led to decreased hardness and impact toughness.
- Samples held at 500 °C and above exhibited an extremely slow isothermal transformation of austenite to bainite, which was not completed within the specified time interval. The remaining stabilised austenite transformed completely into martensite on cooling to room temperature. The sample held at 500 °C, which contained upper bainite and fresh martensite, exhibited the lowest impact toughness.
- Despite the obvious increase in impact toughness due to the modified heat treatment, it remains relatively low, which is primarily due to the presence of undissolved carbides along the boundaries of the former austenitic crystal grains. The hardness of austempered samples is also low, indicating the potential benefits of additional tempering to improve hardness and impact toughness.

These conclusions illustrate the complex relationship between isothermal heat treatment, microstructure, hardness, and impact toughness in the hot-work tool steel investigated and highlight opportunities for further optimisation in order to achieve better mechanical properties.

Author Contributions: Conceptualization, A.B. and J.B.; methodology, A.B. and J.B.; validation, A.B., J.B. and T.B.; formal analysis, A.B. and B.Š.B.; investigation, A.B.; writing—original draft preparation, A.B.; writing—review and editing, J.B. and T.B.; visualization, A.B. and B.Š.B.; supervision, J.B. All authors have read and agreed to the published version of the manuscript.

Data Availability Statement: The data presented in this study are available in the article.

References

1. Mesquita, R.A. *Tool Steels: Properties and Performance*; CRC Press: Boca Raton, FL, USA, 2016.
2. Roberts, G.; Krauss, G.; Kennedy, R. *Tool Steels*, 5th ed.; ASM International: Almere, The Netherlands, 1998.
3. Davis, J.R. (Ed.) *ASM Speciality Handbook—Tool Materials*; ASM International: Almere, The Netherlands, 1995.
4. Caliskanoglu, D.; Siller, I.; Ebner, R.; Leitner, H.; Jeglitsch, F.; Waldhauser, W. Thermal Fatigue and Softening Behavior of Hot Work Tool Steels. In Proceedings of the 6th International Tooling Conference, Karlstad, Sweden, 10–13 September 2002; pp. 707–719.
5. Podgornik, B.; Leskovšek, V. Microstructure and Origin of Hot-Work Tool Steel Fracture Toughness Deviation. *Metall. Mater. Trans. A Phys. Metall. Mater. Sci.* **2013**, *44*, 5694–5702. [CrossRef]
6. Persson, A.; Hogmark, S.; Bergström, J. Simulation and Evaluation of Thermal Fatigue Cracking of Hot Work Tool Steels. *Int. J. Fatigue* **2004**, *26*, 1095–1107. [CrossRef]
7. Pellizzari, M.; Massignani, D.; Amirabdollahian, S.; Deirmina, F. Thermal Fatigue Behavior of AISI H13 Hot Work Tool Steel Produced by Direct Laser Metal Deposition. *Steel Res. Int.* **2023**, *94*, 2200449. [CrossRef]
8. Fuchs, K.D. Hot-Work Steels with Improved Properties for Diecasting Applications. In Proceedings of the 6th International Tooling Conference, Karlstad, Sweden, 10–13 September 2002; pp. 17–26.
9. Imbert, C.A.C.; McQueen, H.J. Hot Ductility of Tool Steels. *Can. Metall. Q.* **2001**, *40*, 235–244. [CrossRef]
10. Wang, G.; Li, Y. Effects of Alloying Elements and Temperature on Thermal Conductivity of Ferrite. *J. Appl. Phys.* **2019**, *126*, 125118. [CrossRef]
11. Hafenstein, S.; Werner, E.; Wilzer, J.; Theisen, W.; Weber, S.; Sunderkötter, C.; Bachmann, M. Influence of Temperature and Tempering Conditions on Thermal Conductivity of Hot Work Tool Steels for Hot Stamping Applications. *Steel Res. Int.* **2015**, *86*, 1628–1635. [CrossRef]
12. Valls, I.; Hamasaiid, A.; Padré, A. High Thermal Conductivity and High Wear Resistance Tool Steels for Cost-Effective Hot Stamping Tools. *J. Phys. Conf. Ser.* **2017**, *896*, 012046. [CrossRef]
13. Kaschnitz, E.; Hofer, P.; Funk, W. Thermophysical Properties of a Hot-Work Tool-Steel with High Thermal Conductivity. *Int. J. Thermophys.* **2013**, *34*, 843–850. [CrossRef]
14. Grabnar, K.; Burja, J.; Balasko, T.; Nagode, A.; Medved, J. The Influence of Nb, Ta and Ti Modification on Hot-Work Tool-Steel Grain Growth during Austenitization. *Mater. Tehnol.* **2022**, *56*, 331–338. [CrossRef]
15. Burja, J.; Nagode, A.; Medved, J.; Balasko, T.; Grabnar, K. Effect of Microalloying on Temperng of Mo-W High Thermal Conductivity Steel. *Metall. Ital.* **2023**, *114*, 22–27.
16. Mayer, S.; Scheu, C.; Leitner, H.; Clemens, H.; Siller, I. Influence of the Cooling Rate on the Mechanical Properties of a Hot-Work Tool Steel. *Berg-Und Hüttenmännische Monatshefte* **2007**, *152*, 132–136. [CrossRef]
17. Okuno, T. Effect of Microstructure on the Toughness of Hot Work Tool Steels, Aisi H13, H10, and H19. *Trans. Iron Steel Inst. Jpn.* **1987**, *27*, 51–59. [CrossRef]
18. Sjöstrom, J.; Bergström, J. Thermal Fatigue Testing of Chromium Martensitic Hot-Work Tool Steel after Different Austenitizing Treatments. *J. Mater. Process. Technol.* **2004**, *153–154*, 1089–1096. [CrossRef]
19. Wang, Y.; Huang, C.; Ma, X.; Zhao, J.; Guo, F.; Fang, X.; Zhu, Y.; Wei, Y. The Optimum Grain Size for Strength-Ductility Combination in Metals. *Int. J. Plast.* **2023**, *164*, 103574. [CrossRef]
20. Mayer, S.; Scheu, C.; Leitner, H.; Siller, I.; Clemens, H. Correlation between Heat Treatment, Microstructure and Mechanical Properties of a Hot-Work Tool Steel. *Int. J. Mater. Res.* **2009**, *100*, 86–91. [CrossRef]
21. Wen, T.; Hu, X.; Song, Y.; Yan, D.; Rong, L. Carbides and Mechanical Properties in a Fe-Cr-Ni-Mo High-Strength Steel with Different V Contents. *Mater. Sci. Eng. A* **2013**, *588*, 201–207. [CrossRef]
22. Im, Y.R.; Oh, Y.J.; Lee, B.J.; Hong, J.H.; Lee, H.C. Effects of Carbide Precipitation on the Strength and Charpy Impact Properties of Low Carbon Mn-Ni-Mo Bainitic Steels. *J. Nucl. Mater.* **2001**, *297*, 138–148. [CrossRef]
23. Bhadeshia, H.K.D.H. *Bainite in Steels: Transformations, Microstructure and Properties*, 2nd ed.; IOM Communications Ltd.: London, UK, 2001.

24. Wang, T.S.; Yang, J.; Shang, C.J.; Li, X.Y.; Zhang, B.; Zhang, F.C. Microstructures and Impact Toughness of Low-Alloy High-Carbon Steel Austempered at Low Temperature. *Scr. Mater.* **2009**, *61*, 434–437. [CrossRef]
25. Krull, H.G.; van Soest, F.; Niederhofer, P.; Schneiders, T. Hot Working Tool Steel with Bainitic Microstructure—The Mechanical Properties at Elevated Temperature. *Steel Res. Int.* **2023**, *94*, 2200329. [CrossRef]
26. Caballero, F.G.; Roelofs, H.; Hasler, S.; Capdevila, C.; Chao, J.; Cornide, J.; Garcia-Mateo, C. Influence of Bainite Morphology on Impact Toughness of Continuously Cooled Cementite Free Bainitic Steels. *Mater. Sci. Technol.* **2012**, *28*, 95–102. [CrossRef]
27. Abbaszadeh, K.; Saghafian, H.; Kheirandish, S. Effect of Bainite Morphology on Mechanical Properties of the Mixed Bainite-Martensite Microstructure in D6AC Steel. *J. Mater. Sci. Technol.* **2012**, *28*, 336–342. [CrossRef]
28. Tartaglia, J.M.; Lazzari, K.A.; Hui, G.P.; Hayrynen, K.L. A Comparison of Mechanical Properties and Hydrogen Embrittlement Resistance of Austempered vs Quenched and Tempered 4340 Steel. *Metall. Mater. Trans. A Phys. Metall. Mater. Sci.* **2008**, *39*, 559–576. [CrossRef]
29. Wei, Z.; Wang, W.; Liu, M.; Tian, J.; Xu, G. Comparison of Wear Performance of Bainitic and Martensitic Structure with Similar Fracture Toughness and Hardness at Different Wear Conditions. *Wear* **2023**, *512–513*, 204512. [CrossRef]
30. Tian, J.; Xu, G.; Zhou, M.; Hu, H. Refined Bainite Microstructure and Mechanical Properties of a High-Strength Low-Carbon Bainitic Steel Treated by Austempering Below and Above MS. *Steel Res. Int.* **2018**, *89*, 1700469. [CrossRef]
31. Sajjadi, S.A.; Zebarjad, S.M. Isothermal Transformation of Austenite to Bainite in High Carbon Steels. *J. Mater. Process. Technol.* **2007**, *189*, 107–113. [CrossRef]
32. Morawiec, M.; Ruiz-Jimenez, V.; Garcia-Mateo, C.; Jimenez, J.A.; Grajcar, A. Study of the Isothermal Bainitic Transformation and Austenite Stability in an Advanced Al-Rich Medium-Mn Steel. *Arch. Civ. Mech. Eng.* **2022**, *22*, 152. [CrossRef]
33. Pashangeh, S.; Banadkouki, S.S.G.; Somani, M.; Kömi, J. Characteristics and Kinetics of Bainite Transformation Behaviour in a High-Silicon Medium-Carbon Steel above and below the M_s Temperature. *Materials* **2022**, *15*, 539. [CrossRef]
34. Guo, H.; Feng, X.; Zhao, A.; Li, Q.; Ma, J. Influence of Prior Martensite on Bainite Transformation, Microstructures, and Mechanical Properties in Ultra-Fine Bainitic Steel. *Materials* **2019**, *12*, 527. [CrossRef]
35. Vončina, M.; Balaško, T.; Medved, J.; Nagode, A. Interface Reaction between Molten Al99.7 Aluminum Alloy and Various Tool Steels. *Materials* **2021**, *14*, 7708. [CrossRef]
36. Uddeholms AB Uddeholm Dievar®. Available online: https://www.uddeholm.com/app/uploads/sites/41/2017/09/Tech-Uddeholm-Dievar-EN.pdf (accessed on 20 November 2023).
37. Zhou, S.B.; Hu, F.; Zhou, W.; Cheng, L.; Hu, C.Y.; Wu, K.M. Effect of retained austenite on impact toughness and fracture behavior of medium carbon submicron-structured bainitic steel. *J. Mater. Res. Technol.* **2021**, *14*, 1021–1034. [CrossRef]